ACCOUNTS
of chemical research

UV Raman Spectroscopic Studies on Active Sites and Synthesis Mechanisms of Transition Metal-Containing Microporous and Mesoporous Materials

FENGTAO FAN,[†,‡] ZHAOCHI FENG,[†] AND CAN LI*[,†]

[†]*State Key Laboratory of Catalysis, Dalian Institute of Chemical Physics,*
[‡]*Graduate University, Chinese Academy of Sciences, 457 Zhongshan Road, Dalian 116023, China*

RECEIVED ON JULY 20, 2009

CONSPECTUS

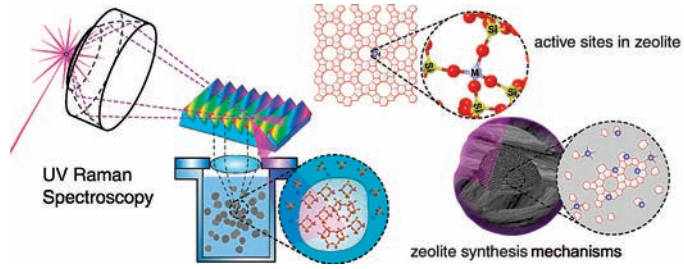

Microporous and mesoporous materials are widely used as catalysts and catalyst supports. Although the incorporation of transition metal ions into the framework of these materials (by isomorphous substitution of Al and Si) is an effective means of creating novel catalytic activity, the characterization of the transition metal species within these materials is difficult. Both the low concentration of the highly dispersed transition metal and the coexistence of extraframework transition metal species present clear challenges. Moreover, the synthetic mechanisms that operate under the highly inhomogeneous conditions of hydrothermal synthesis are far from well understood.

A useful technique for addressing these challenges is UV Raman spectroscopy, which is a powerful technique for catalyst characterization and particularly for transition metal-containing microporous and mesoporous materials. Conventional Raman spectroscopy, using visible and IR wavelengths, often fails to provide the information needed for proper characterization as a result of fluorescence interference. But shifting the excitation source to the UV range addresses this difficulty: interference from fluorescence (which typically occurs at 300−700 nm or greater) is greatly diminished. Moreover, signal intensity is enhanced because Raman intensity is proportional to the fourth power of the scattered light frequency.

In this Account, we review recent advances in UV Raman spectroscopic characterization of (i) highly dispersed transition metal oxides on supports, (ii) transition metal ions in the framework of microporous and mesoporous materials, and (iii) the synthetic mechanisms involved in making microporous materials. By taking advantage of the strong UV resonance Raman effect, researchers have made tremendous progress in the identification of isolated transition metal ions incorporated in the framework of microporous and mesoporous materials such as TS-1, Ti-MCM-41, Fe-ZSM-5, and Fe-SBA-15. The synthetic mechanisms involved in creating microporous materials (such as Fe-ZSM-5 and zeolite X) have been investigated with resonance and *in situ* UV Raman spectroscopy. The precursors and intermediates evolved in the synthesis solution and gels can be sensitively detected and followed during the course of zeolite synthesis. This work has resulted in a greater understanding of the structure of transition metal-containing microporous and mesoporous materials, providing a basis for the rational design and synthesis of microporous and mesoporous catalysts.

Introduction

Isomorphous substitution of the aluminum and silicon in microporous and mesoporous materials with other elements, particularly transition metals, is considered one of the most effective ways to modify the physicochemical properties of microporous and mesoporous materials.[1] Transition metal incorporated microporous and mesoporous materials such as Fe-ZSM-5, TS-1, and Ti-MCM-41 have been successfully applied in a

Published on the Web 12/22/2009 www.pubs.acs.org/acr
10.1021/ar900210g

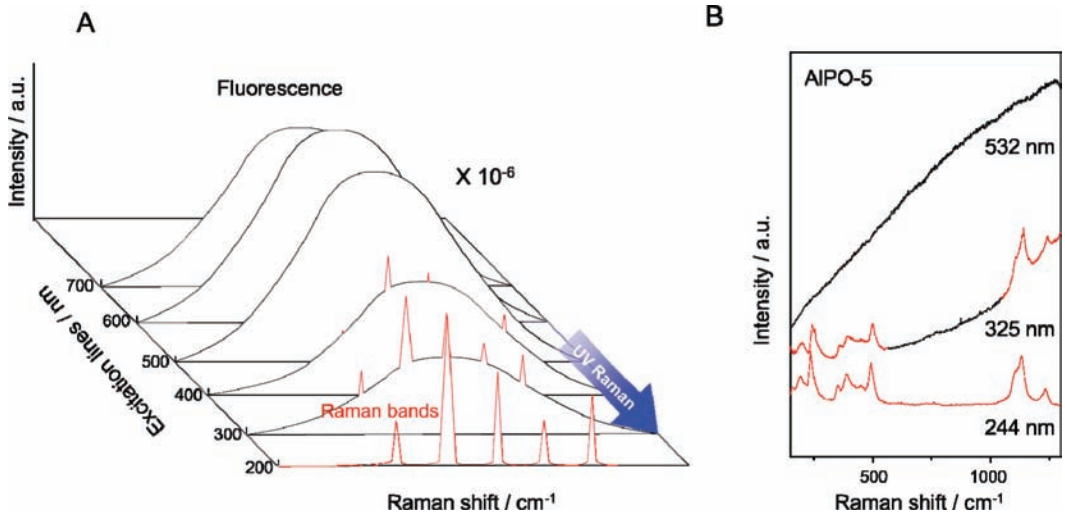

FIGURE 1. (A) Schematic description of the fluorescence bands appearing mostly in the visible region from about 300 to 700 nm, and the Raman signal is usually obscured by the strong fluorescence interference. To avoid fluorescence interference in the Raman spectrum, the Raman spectrum is shifted from the visible region to the UV region ($\lambda < 300$ nm), by shifting the excitation laser from the visible region to the UV region. (B) Raman spectra of AlPO4-5 excited at 244, 325, and 532 nm.

number of catalytic processes.[2−6] The catalytic properties of transition metal substituted microporous and mesoporous materials depend largely on their composition and structure. A deep understanding of the structure of active metal species and the formation mechanism in microporous materials is helpful for developing zeolite-based catalysts with high selectivity and activity.[7,8] However, it is hard to obtain definite information on the transition metal ions in these materials, such as their coordination environments and distributions, because of their low concentration.

Raman spectroscopy is potentially a powerful technique for characterizing the microporous and mesoporous materials. Unfortunately conventional Raman spectroscopy often fails due to strong fluorescence interference caused by organic templates, impurities, and surface defect sites.[9] Fluorescence spectra are usually in the range from 300 to 700 nm or longer, but there exists a cutoff wavelength in the shorter wavelength side in the UV region for condensed materials. Fluorescence interference can be avoided in Raman spectra if the excitation source is shifted from the visible region to the UV region, as described in Figure 1A. Figure 1B shows the Raman spectra of $AlPO_4$-5 excited at 244, 325, and 532 nm. The spectral features obtained by the excitation at 532 nm have been obscured by strong fluorescence. When the excitation line shifts to 325 nm, Raman signal with a weak fluorescence background can be obtained. In contrast, a well-resolved spectrum of $AlPO_4$-5, with high signal-to-noise, can be obtained with 244 nm excitation. In addition, because the normal Raman scattering intensity is proportional to the fourth power of the scattered light frequency, the sensitivity of UV Raman is much higher than that of visible or near-IR Raman spectroscopy.

Another important advantage of using UV light in Raman spectroscopy is a significant improvement in resonance enhancement. The Raman scattering intensity is proportional to $|\alpha_{\rho\sigma}|^2$, and the polarizability, $\alpha_{\rho\sigma}$, can be calculated according to the Kramers−Heisenberg equation,[10]

$$(\alpha_{\rho\sigma})_{mn} = \frac{1}{h}\sum_r \left[\frac{M_{me}M_{en}}{\Delta E_{me} - h\nu_0 + i\Gamma_r} + \frac{M_{me}M_{en}}{\Delta E_{en} + h\nu_0 + i\Gamma_r}\right] \quad (1)$$

In eq 1, ν_0 is the frequency of the excitation laser, ΔE_{me} stands for the energy difference between the two electronic states m and e, while state n is the first excited vibrational energy level. The polarizability, $\alpha_{\rho\sigma}$, would be greatly increased when the laser line, $h\nu_0$, is close to an electronic transition, ΔE_{me}.[11] As a result, the cross section of Raman scattering could be considerably enhanced. The Raman intensity can be increased dramatically. A resonance-enhanced signal can be several orders of magnitude more intense than the normal Raman signal.[10] Resonance Raman spectroscopy is particularly useful when applied to a sample containing a mixture of individual species.[12] Raman bands associated with different components can be selectively enhanced when excited according to their electronic transitions.

Transition metal ions substituted into the framework of microporous and mesoporous materials show a charge transfer transition between transition metal ions and the framework oxygen ions, usually in the UV region, for example, 250 nm for Fe-ZSM-5, 220 nm for TS-1, and 280 nm for V-MCM-

41. Accordingly, the characteristic bands directly associated with the framework transition metal ions can be enhanced by exciting these transition metal ions with UV lasers. Therefore, it is possible to identify isolated framework transition metal ions in microporous and mesoporous materials.

Understanding the synthesis mechanism of the microporous and mesoporous materials is one of the challenging chemical problems today. Although numerous zeolitic structures have successfully been synthesized, rational design and synthesis remains elusive. Such an approach requires a full understanding of the crystallization process and the formation mechanism of zeolites.[13] A few studies have addressed the preparation of zeolites, and several assembly mechanisms regarding the nucleation and crystal growth have been proposed,[14−16] including the formation and consumption of small primary units, medium nuclei, and large crystals.[17,18] However, it is difficult to study the detailed mechanisms of the zeolitic formation due to the extreme complexity of hydrothermal crystallizations.[19] More specifically, most studies were performed by ex-situ technique, namely, frequently removing aliquots of the reaction mixture and analyzing the samples after quenching the reaction. However, microporous zeolite-type materials are usually synthesized under hydrothermal conditions, and the need for sample quenching and workup may cause dramatic and undeterminable structural changes.[20]

In situ characterization under working conditions is a powerful method to probe the entire sequence of species formed during zeolite synthesis without the need for quenching. This not only greatly simplifies experimental procedures but also allows for unfettered observation of the true synthetic intermediates. However, *in situ* characterization of zeolite synthesis remains relatively unexplored.[21,22] Raman spectroscopy is a suitable technique to investigate aqueous solutions as well as solid phases of zeolite synthesis mixtures due to the low Raman scattering cross section of water. In particular, UV Raman spectroscopy avoids strong fluorescence interference caused by template decomposition under hydrothermal conditions.[23] In addition, UV Raman can sensitively and selectively detect framework transition metal ions due to strong resonance Raman enhancement. These advantages render UV Raman an excellent tool for the *in situ* study of zeolite formation.

During the past decade, we have used UV Raman spectroscopy to study transition metal-containing microporous and mesoporous materials such as TS-1, Ti-MCM-41, Fe-ZSM-5, and Fe-SBA-15 in an effort to elucidate the structure of active sites and synthesis mechanism of these materials. Recently, in an effort to gain a detailed understanding of the formation mechanism of microporous materials, we have developed methods for the direct observation of hydrothermal reactions by *in situ* UV Raman spectroscopy. The building blocks from the intermediate to the final crystals were well identified by taking the advantage of this powerful technique.

UV Raman Characterization of Transition Metal-Containing Microporous and Mesoporous Materials

Identification of Framework Ti Sites in TS-1 and Ti-MCM-41. TS-1 exhibits a remarkably high catalytic efficiency and selectivity in olefin epoxidation, phenol hydroxylation, and secondary alcohol dehydrogenation using H_2O_2 as oxidant.[24] It has been one of the most heavily studied heterogeneous catalysts in recent years.[8] However, the structure of the active site has not been definitively identified due to the extremely low concentration of the titanium site in the framework, although TS-1 has been extensively characterized by various techniques.[25−27]

The charge transfer of $p\pi-d\pi$ transition between oxygen and titanium atoms in the framework of TS-1 was observed at 220 nm in the UV−visible diffuse reflectance spectrum (Figure 2A). The laser line at 244 nm was chosen to excite the electronic transition absorption of the Ti species in TS-1 for the Raman spectrum (Figure 2B). Besides the characteristic bands at 380 and 800 cm^{-1} for the MFI zeolite lattice, three new bands at 490, 530, and 1125 cm^{-1} were observed in the UV Raman spectrum of TS-1. The appearance of these bands are associated with framework Ti but not with silicalite-1.[28] The resonance Raman bands at 490, 530, and 1125 cm^{-1} can be attributed to a local unit of $[Ti(OSi)_4]$ of TS-1, denoted by Ti−O−Si. The bands at 490 and 530 cm^{-1} are ascribed to the bending and symmetric stretching vibration of the framework Ti−O−Si species, respectively. The band at 1125 cm^{-1} is assigned to the asymmetric stretching vibration of Ti−O−Si.[29]

In the Raman spectrum of TS-1 excited at 325 and 488 nm (Figure 2B), three additional bands at 144, 390, and 637 cm^{-1} are observed, which can be assigned to extraframework TiO_2 (anatase). However, these bands are relatively weak in the UV Raman spectrum excited at 244 nm. This phenomenon can be explained in terms of nonradiation and fluorescence processes in the TiO_2 when excited with UV light.[29]

UV resonance Raman spectra of Ti-MCM-41 are shown in Figure 3A. Three additional Raman bands at 482, 520, and 1110 cm^{-1} are observed in the spectrum of Ti-MCM-41 when compared with that of MCM-41. These bands are attributed to tetrahedrally coordinated Ti species in the amorphous wall of

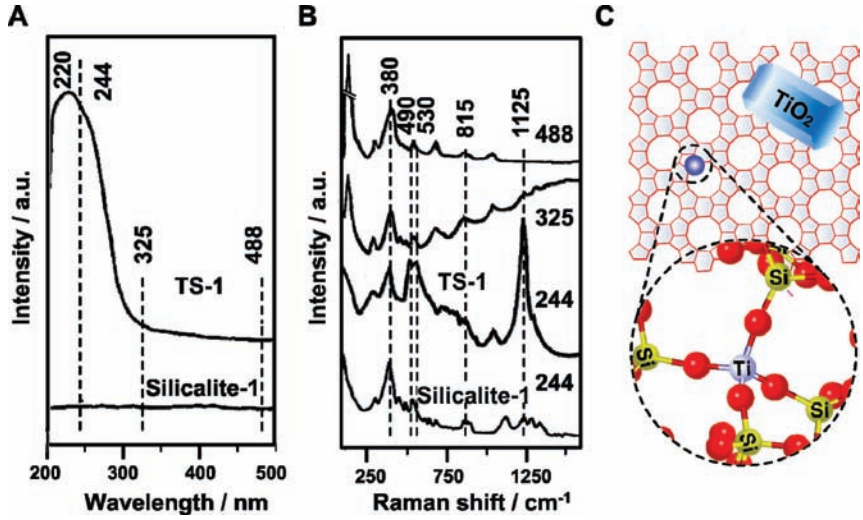

FIGURE 2. (A) UV−visible diffuse reflectance spectra and (B) Raman spectra excited with different laser lines at 244, 325, and 532 nm of silicalite-1 and TS-1[28,29] and (C) a schematic description of the titanium site in the framework of TS-1.

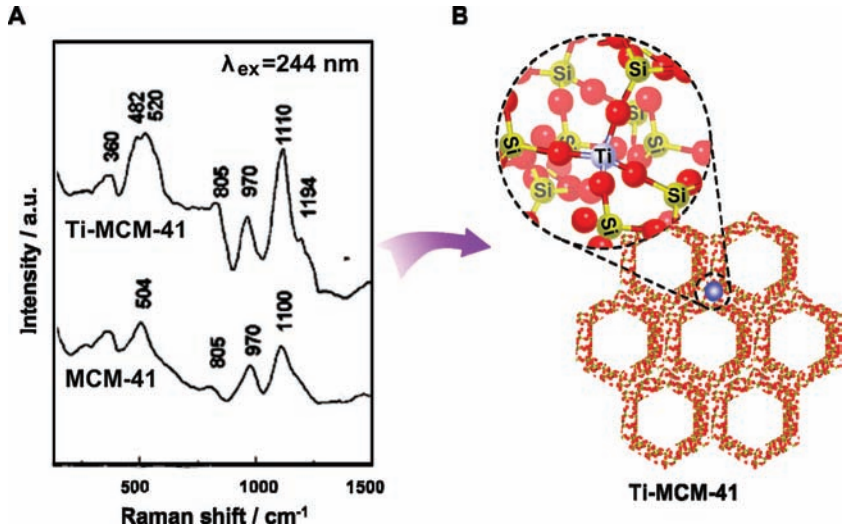

FIGURE 3. (A) UV Raman spectra of MCM-41 and Ti-MCM-41 (Si/Ti = 200) excited with 244 nm and (B) a schematic description of the titanium sites in the framework of MCM-41.

Ti-MCM-41.[31] The fact that the frequency of the characteristic band at 1110 cm^{-1} of Ti-MCM-41 is lower than that of TS-1 (1125 cm^{-1}) indicates that the coordination environment of Ti atoms in Ti-MCM-41 and TS-1 is different. The Ti atoms in TS-1 are fixed in the rigid framework sites, and the Ti atoms in Ti-MCM-41 are relatively flexible,[30,31] while the highly dispersed titanium species on the SiO_2 surface (prepared by chemical grafting) are flexible and possess a distorted tetrahedral coordination geometry.

Figure 4 compares the three coordination environments of titanium sites and the corresponding UV Raman bands at ~1125, 1100, and 1085 cm^{-1}, respectively, for TS-1, Ti-MCM-41, and Ti/SiO_2. The characteristic frequency of Ti−O−Si is sensitive to the coordination environment. The red shift from 1125 cm^{-1} for rigid tetrahedral coordination of the titanium site in TS-1 to 1085 cm^{-1} for very flexible coordination of titanium sites on SiO_2 can be used as a figure of merit in assessing the coordination geometry of Ti^{4+} in microporous and mesoporous materials.[32]

The Identification of the Isolated Iron Sites in Fe-ZSM-5 and Fe-SBA-15. Isomorphous substitution of the aluminum and silicon in microporous and mesoporous materials with trace quantities of trivalent elements changes the acidity and catalytic properties. Iron-exchanged microporous materials, such as Fe-ZSM-5 and Fe-SBA-15, have been successfully applied in numerous catalytic processes.[33−35]

Figure 5A shows the UV−visible diffuse reflectance spectra of Fe-ZSM-5. The strong absorption band at 263 nm is assigned to the charge transfer of pπ−dπ transition between oxygen and iron atoms in the framework of Fe-ZSM-5, while

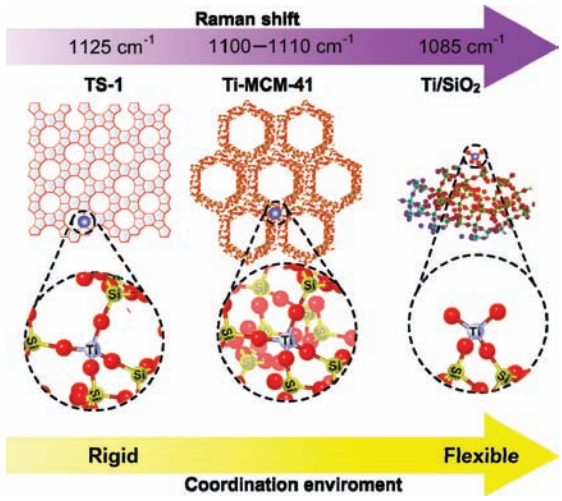

FIGURE 4. Characteristic Raman frequencies in UV Raman spectra of TS-1, Ti-MCM-41, and Ti/SiO_2 and the schematic description of the coordination environments of the titanium ions.

four bands at 376, 413, 438, and 480 nm come from the d–d transitions of iron atoms in tetrahedral coordination environments. These bands are direct evidence of the existence of framework iron ions in zeolites. The above analysis was substantiated by projected density of state (PDOS) calculations of the framework Fe tetrahedron in Fe-ZSM-5 using DFT (Figure 5B).[36]

Figure 5C shows the UV Raman spectra of ZSM-5 and Fe-ZSM-5 excited at 244 nm, which is close in energy to the charge transfer band of Fe-ZSM-5. The UV Raman spectrum of Fe-ZSM-5 exhibits new bands at 516, 1016, 1115, and 1165 cm^{-1} when excited at 244 nm. The Raman bands at 516, 1115, and 1165 cm^{-1} become considerably weaker when sample is excited at 325 nm and disappear when it is excited at 532 nm. The bands at 516 and 1115 cm^{-1} are resonance enhanced and attributed to the symmetric and asymmetric stretching vibrations of the framework Fe–O–Si species in tetrahedral coordination (Figure 5D). Notably, the band at 1016 cm^{-1} is observed regardless of excidation wavelength. This band is not a resonance Raman band and is associated with the Si–O–Si bond near framework iron as shown in Figure 5D.[37,38]

The band at 1165 cm^{-1} is a resonance Raman band and can be excited with laser of 244 nm. Periodic DFT calculation confirms that this band is asymmetric stretching vibrations of the framework Fe–O–Si.[36] This vibration mode is

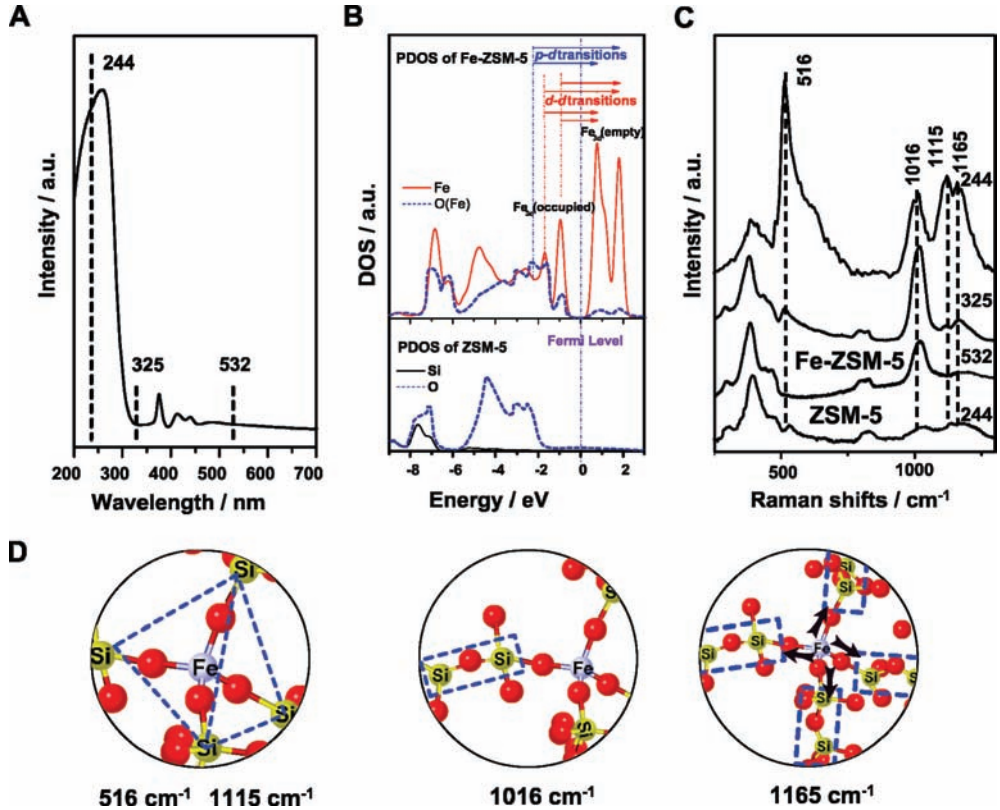

FIGURE 5. (A) UV–visible diffuse reflectance spectra of Fe-ZSM-5, (B) calculated projected density of states (PDOS) of the Fe and coordinated O ions in Fe-ZSM-5 and for Si and coordinated O ions in ZSM-5, (C) Raman spectra of Fe-ZSM-5 with excitation lines at 244, 325, and 532 nm and Raman spectra of ZSM-5 excited at 244 nm, and (D) schematic showing the different vibration models of the Raman bands at 516, 1016, 1115, and 1165 cm^{-1}.[36,41]

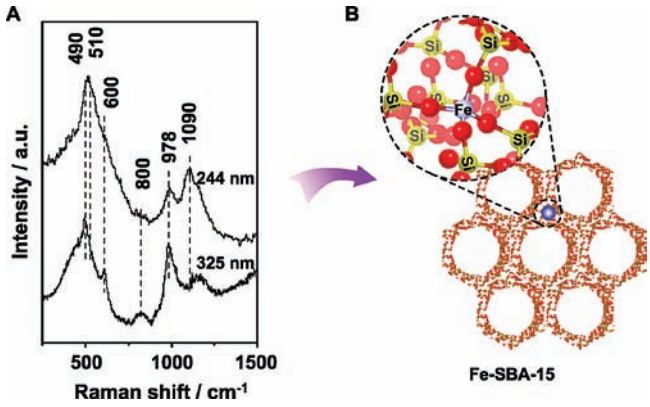

FIGURE 6. (A) UV resonance Raman spectra of Fe-SBA-15 excited with 244 and 325 nm and (B) a schematic description of the iron site in the framework of MCM-41.[39]

driven by the stretching of four neighboring framework Si−O−Si bonds as shown in Figure 5D. In another words, the intensity of this band relates to the crystallinity of the zeolite framework.

To investigate the different coordination environments of the framework Fe species in mesoporous materials, Fe-SBA-15 samples were studied by UV Raman spectroscopy. Figure 6 shows the UV Raman spectra of Fe-SBA-15 excited with the lasers at 244 and 325 nm. Two strong Raman bands at 510 and 1090 cm^{-1} are detected for Fe-SBA-15 when excited with 244 nm. These bands are assigned to the symmetric and asymmetric Fe−O−Si stretching modes of the amorphous silica framework of Fe-SBA-15.[39] The Raman spectrum of Fe-SBA-15 excited with 325 nm shows only a strong Raman band at 978 cm^{-1}, which can be also seen in the Raman spectra excited with 244 nm. Obviously, this Raman band is a nonresonance Raman band and is associated with the Si−O−Si bond near framework iron species.[39]

In summary, there are four characteristic bands at 516, 1016, 1115, and 1165 cm^{-1} for Fe-ZSM-5, while only three bands at 510, 978, and 1090 cm^{-1} are observed for Fe-SBA-15, which suggests that coordination environments of the framework iron differ between the materials. The red shift from 1115 cm^{-1} for rigid tetrahedral coordination of iron in Fe-ZSM-5 to 1090 cm^{-1} for flexible coordination of iron sites in Fe-SBA-15 has a similar trend to that for the titanium sites in TS-1 and Ti-MCM-41. These results are very useful for evaluating the coordination geometry of transition metal ions incorporated in the microporous and mesoporous materials.

UV Raman Spectroscopic Study on the Crystalization of Microporous Materials

Synthesis Mechanism of Fe-ZSM-5: From Molecular Fragments to Crystals. In order to understand how framework Fe atoms incorporate into the zeolite framework sites, the crystallization processes of Fe-ZSM-5 were characterized by UV Raman spectroscopy. As we have previously mentioned, information on the framework structure and the coordination environment of iron species can be selectively obtained by shifting the excitation wavelength from 325 to 244 nm.

The UV Raman spectra of Fe-ZSM-5 (λ_{ex} = 325 nm) at various synthesis times are shown in Figure 7A. The Raman spectrum of the initial precursor is characterized by two broad bands centered at 460 and 984 cm^{-1}, which have been assigned to ν_s(Si−O−Si) of five- and six-membered silicate rings[40] and ν_s(Si−O−Si) near framework iron species, respectively.[37,38] After hydrothermal synthesis begins, the bands at 460 and 984 cm^{-1} become sharp, while the latter shifts to a higher frequency. The increasing intensity of the

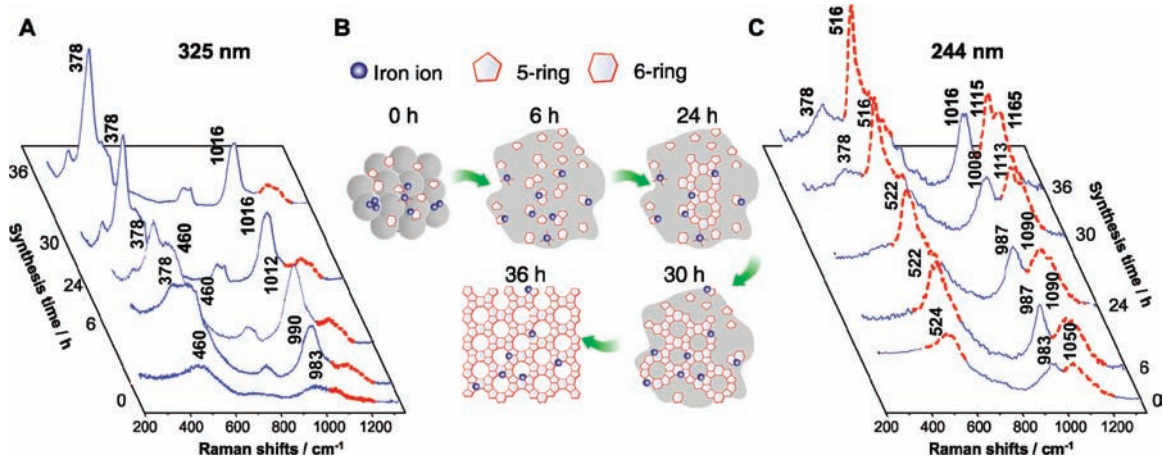

FIGURE 7. UV resonance Raman spectra of Fe-ZSM-5 (Si/Fe = 152) excited at (A) 325 nm and (C) 244 nm for different crystallization stages at various time of synthesis and (B) a proposed scheme for the formation mechanism of Fe-ZSM-5.

broad band centered at 460 cm^{-1} indicates that the silicate rings are formed within the gel upon hydrothermal treatment.

With further synthesis time for 24 h, the Raman spectra show characteristic bands of the MFI structure at 380 cm^{-1} with a comparatively weak broad band centered at 460 cm^{-1}. This suggests the formation of a large quantity of MFI crystals. The Raman band in the amorphous gel at 460 cm^{-1} becomes undetectable for the sample crystallized for 30 and 36 h. The Raman band at 983 cm^{-1} of the precursor shifts to a higher frequency throughout the entire synthesis process and appears at 1016 cm^{-1} after crystallization for 36 h, indicating the Si−O−Si bonds near the iron species in tetrahedral coordination become rigid.

The excitation wavelength, $\lambda_{ex} = 244$ nm, was used, and the process described above was repeated to monitor the evolution of the iron species during the synthesis process (Figure 7C). Upon hydrothermal treatment, the broad band at 524 cm^{-1} becomes sharp and strong and shifts to a lower frequency at 516 cm^{-1}. The bands at 983 and 1060 cm^{-1} shift to higher frequencies at 1016 and 1115 cm^{-1}, respectively. These results indicate the existence of tetrahedrally coordinated [$Fe(OSi)_4$] units in the early stages of Fe-ZSM-5 formation, whereas they are not as rigidly coordinated as those in a well-crystallized zeolite framework.[41] A Raman band at 1165 cm^{-1} appears as a shoulder of the band at 1080 cm^{-1} in the Raman spectrum of sample after 6 h of synthesis time and then becomes narrow and strong with increasing crystallinity. The evolution of the Raman band at 1165 cm^{-1} agrees with our periodic DFT assignment, demonstrating that this vibrational mode is strongly influenced by zeolite framework crystallinity.[36,41]

The rate of hypsochromic shift of the band at 983 cm^{-1} when $\lambda_{ex} = 244$ nm is slower than when $\lambda_{ex} = 325$ nm. In addition, the characteristic Raman bands of the MFI structure at 380 and 800 cm^{-1} appear much later in the Raman spectra when $\lambda_{ex} = 244$ nm (Figure 7C, 30 h) than when $\lambda_{ex} = 325$ nm (Figure 7A, 18 h). Our previous work has shown that UV Raman spectroscopy is more sensitive to the surface phase of a solid sample when the sample absorbs UV light.[42,43] It should be noted that all the sample particles at various time intervals during the synthesis of Fe-ZSM-5 have strong absorbance below 300 nm.[41] Thus, the Raman scattering signal excited by 244 nm laser is mainly from the skin region of the sample particles, while that excited by 325 nm reflects the overall information from the whole particle. These results suggest that crystalline Fe-ZSM-5 forms from a core of sample particles and then develops from the inside out, as was confirmed by HRTEM.[41]

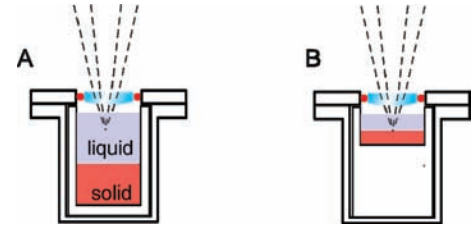

FIGURE 8. (A) Sample holder and the focus point of *in situ* Raman cell for liquid phase study, and (B) sample holder and the focus point of *in situ* Raman cell for solid phase study.[45]

The proposed synthesis mechanism of Fe-ZSM-5 is shown in Figure 7B. Crystalline Fe-ZSM-5 is formed by the aggregation and nucleation of the distorted tetrahedrally coordinated [$Fe(OSi)_4$] species and five- and six-membered silicate rings, which are formed in the early stages of the synthesis process. The nucleation takes place in the core of the amorphous phase. Crystalline Fe-ZSM-5 develops into larger crystals by consuming the iron species in distorted tetrahedral coordination and silicate species in the amorphous shell and ultimately becomes well-crystallized sample.

The Synthesis Mechanism of Zeolite X. UV Raman spectroscopy can provide molecular information from aqueous solutions to solid phases of zeolite synthesis mixtures due to the low Raman scattering cross section of water. More specifically, UV Raman spectroscopy can provide structural information from the small precursor units to the large crystals during the zeolite formation process due to decreased fluorescence and increasing sensitivity. These advantages make UV Raman a potentially suitable tool for the *in situ* study of the mechanism of zeolite framework formation.[44]

In an effort to gain a greater understanding of hydrothermal synthesis, an *in situ* Raman cell for hydrothermal synthesis of zeolites was designed and coupled to UV Raman spectroscopy.[45] A silicon rubber-sealed lens on top of the cell allows focusing of the laser on the surface of the samples in the cell, which enhances the Raman signal up to 3−4 times that of a plane window. Two types of sample holders with different depth are used to ensure that the laser can be focused on either the liquid phase (Figure 8A) or the interface between liquid and solid phases (Figure 8B).

The hydrothermal synthesis of zeolite X was studied for investigating both the solid and liquid phase under hydrothermal conditions by UV Raman spectroscopy.[45] Two bands were observed in the initial spectrum of the liquid phase at 774 and 920 cm^{-1}, which are attributed to monomeric silicate species in the liquid phase.[46] A plot of the intensity of the band at 774 cm^{-1} is shown in Figure 9B. The result indicates that initially in the gel, the amorphous solid is in equilibrium with the monomeric silicate species in the liquid phase. With the

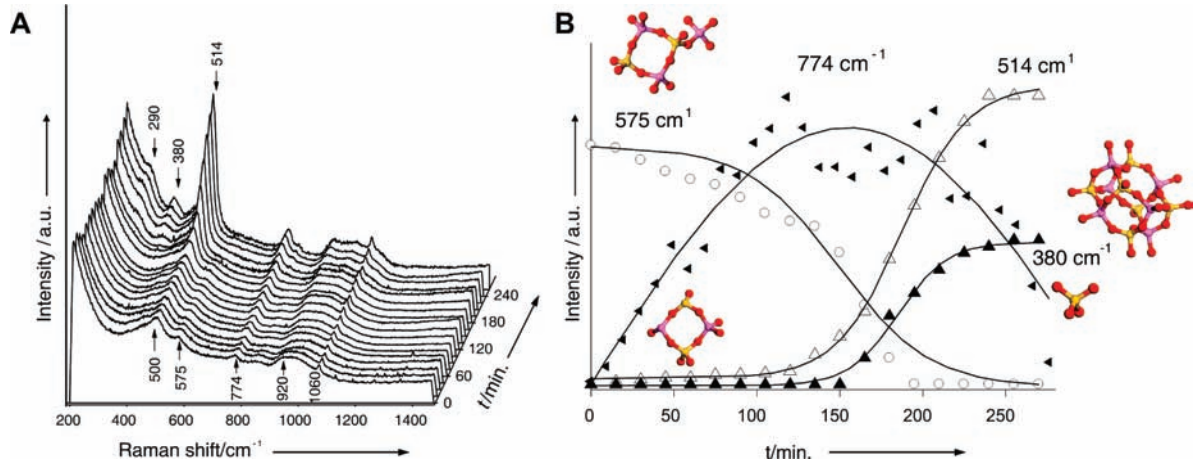

FIGURE 9. (A) In situ UV Raman spectra of solid phase of zeolite X synthesis at 373 K, spectra were collected from 0 to 270 min. Each spectrum was collected at an interval of 10 min. (B) Plot of intensities of the 380, 514, 575, and 774 cm^{-1} bands as a function of time.

increasing temperature, a large amount of monomers are formed from the depolymerization of amorphous precursors. As the reaction proceeds, the growing product crystals require more monomers. Finally, all amorphous precursors are consumed and transformed into crystalline zeolite.

Figure 9A shows *in situ* UV Raman spectra recorded for the solid phase at 373 K under hydrothermal conditions. The sharp band at 500 cm^{-1} in Figure 8 indicates that the gel predominantly consists of four-membered silicate rings.[47,48] Upon heating, this band becomes prominent and gradually shifts to 514 cm^{-1}, assigned to the breathing mode vibration of the four-membered ring in the crystalline framework of zeolite X. The appearance of the two Raman bands at 298 and 380 cm^{-1}, which can be assigned to the bending mode of double six-membered ring, indicate that the formation of the zeolite X framework is directly related to the four-membered ring and six-membered ring species.[49]

The Raman band at 575 cm^{-1} appears at the very beginning of the synthesis, and the intensity decreases with increasing crystallization (Figure 9B). The most interesting phenomenon is that the three bands at 298, 380, and 514 cm^{-1} appear while the band at 575 cm^{-1} disappears. This indicates that the species corresponding to the 575 cm^{-1} band is a key intermediate for the formation of zeolite X. Raman bands between 550 and 600 cm^{-1} have been assigned to Al−O−Si stretches.[50] According to our experiments and theoretical calculations, this band could be attributed to the Si−O−Al stretches on the branches of the ring structure.[45]

Based on *in situ* Raman spectroscopy and DFT calculation, the mechanism of the framework formation of zeolite X is proposed. During hydrothermal synthesis of zeolite X, the amorphous solid phase is dissolved to form the monomer silicate species in the liquid phase, which takes part in the framework formation. The amorphous aluminosilicate species in the early stage of nucleation are composed of predominately four-membered rings, with a small contribution from branched derivatives. Four-membered rings bond with two six-membered rings, together with the monomer silicate species in the liquid phase, to form the crystalline zeolite X framework.

Concluding Remarks and Prospects

UV Raman spectroscopy broadens the application of Raman spectroscopy in the study of microporous and mesoporous materials. Isolated transition metal species in the framework of microporous and mesoporous materials can be identified by UV resonance Raman spectroscopy, even at very low concentrations. The coordination surroundings of framework transition metal ions in microporous and mesoporous materials can be sensitively detected by UV Raman spectroscopy. The crystallization process of zeolite has been successfully studied *in situ* by UV Raman spectroscopy, which can sensitively monitor the precursors and intermediates evolved during the synthesis under working conditions.

We anticipate that in the future progress will be made in the following aspects:

The morphological and structural factors of the catalytic materials, in particular the structure of active centers on catalytic materials, could be elucidated through UV resonance Raman characterization under real catalytic reaction conditions.

In situ UV Raman spectroscopy will play a key role in mechanistic studies of materials synthesis, particularly in hydrothermal synthesis at high pressures and temperatures. *In situ* UV Raman spectroscopy will provide information on the important intermediates, key steps, and optimized parameters for the hydrothermal synthesis of materials.

It is not very risky to predict that based on the knowledge obtained from *in situ* UV Raman spectroscopy, novel catalytic materials could be synthesized by rational design and well-controlled synthesis parameters.

Can Li thanks his former students, Guang Xiong, Bo Han, Yi Yu, Yuxiang Lian, Ying Li, Keju Sun, and Haian Xia for their contribution to this work. This work was financially supported by National Basic Research Program of China (2009CB623507) and National Natural Science Foundation of China (20773118, 20673115).

BIOGRAPHICAL INFORMATION

Fengtao Fan received his B.S. degree in Apply Chemistry in 2003 from Shanxi University, China. He is finishing his doctoral work at the Dalian Institute of Chemical Physics (DICP), Chinese Academy of Sciences, under the direction of Can Li. His work is focused on understanding the mechanism of zeolite synthesis via *in situ* UV Raman spectroscopy.

Zhaochi Feng received his Ph.D. degree from Dalian University of Technology, China, in 1997. He is currently a Professor in DICP. His research interests include laser spectroscopy, such as Raman and UV Raman spectroscopies, laser-induced fluorescence spectroscopy, and theoretical calculations.

Can Li received his Ph.D. degree in 1988 from Dalian Institute of Chemical Physics and was promoted to full professor in 1993. His research interests are (1) vibrational and electronic spectroscopy, especially UV Raman spectroscopies, and their applications in catalysis and materials science, (2) environmental catalysis and green catalysis for fine chemicals, (3) asymmetric catalysis on surfaces and in mesoporous solid catalysts modified with chiral molecules, and (4) energy-related catalysis, photocatalysis, biomass conversion, and water splitting to produce H_2. Now he is director of the state laboratory of catalysis (in DICP), the chairman of the Catalysis Society of China, and the President of the International Association of Catalysis Societies.

FOOTNOTES

*To whom correspondence should be addressed. Tel: 86-411-84379070. Fax: 86-411-84694447. E-mail: canli@dicp.ac.cn (C. Li). Homepage: http://www.canli.dicp.ac.cn.

REFERENCES

1 Hartmann, M.; Kevan, L. Transition-Metal Ions in Aluminophosphate and Silicoaluminophosphate Molecular Sieves: Location, Interaction with Adsorbates and Catalytic Properties. *Chem. Rev.* **1999**, *99*, 635–664.

2 Corma, A. From Microporous to Mesoporous Molecular Sieve Materials and Their Use in Catalysis. *Chem. Rev.* **1997**, *97*, 2373–2420.

3 Long, R. Q.; Yang, R. T. Superior Fe-ZSM-5 Catalyst for Selective Catalytic Reduction of Nitric Oxide by Ammonia. *J. Am. Chem. Soc.* **1999**, *121*, 5595–5596.

4 Parker, W. O.; Millini, R. Ti Coordination in Titanium Silicalite-1. *J. Am. Chem. Soc.* **2006**, *128*, 1450–1451.

5 Sayari, A. Catalysis by Crystalline Mesoporous Molecular Sieves. *Chem. Mater.* **1996**, *8*, 1840–1852.

6 Kosuge, K. Titanium-Containing Porous Silica Prepared by a Modified Sol-Gel Method. *J. Phys. Chem. B* **1999**, *103*, 3563–3569.

7 Ricchiardi, G.; Damin, A.; Bordiga, S.; Lamberti, C.; Spano, G.; Rivetti, F.; Zecchina, A. Vibrational Structure of Titanium Silicate Catalysts. A Spectroscopic and Theoretical Study. *J. Am. Chem. Soc.* **2001**, *123*, 11409–11419.

8 Fan, W. B.; Duan, R. G.; Yokoi, T.; Wu, P.; Kubota, Y.; Tatsumi, T. Synthesis, Crystallization Mechanism, and Catalytic Properties of Titanium-Rich TS-1 Free of Extraframework Titanium Species. *J. Am. Chem. Soc.* **2008**, *130*, 10150–10164.

9 Stair, P. C. *The Application of UV Raman Spectroscopy for the Characterization of Catalysts and Catalytic Reactions*; Advances in Catalysis, Vol. 51; Elsevier Academic Press Inc: San Diego, CA, 2007; pp 75−98.

10 Spiro, T. G. Resonance Raman Spectroscopy. New Structure Probe for Biological Chromophores. *Acc. Chem. Res.* **1974**, *7*, 339–344.

11 Clark, R. J. H.; Dines, T. J. Resonance Raman Spectroscopy and Its Application to Inorganic Chemistry. *Angew. Chem.* **1986**, *98*, 131–160.

12 Xiong, G.; Li, C.; Li, H. Y.; Xin, Q.; Feng, Z. C. Direct Spectroscopic Evidence for Vanadium Species in V-MCM-41 Molecular Sieve Characterized by UV Resonance Raman Spectroscopy. *Chem. Commun.* **2000**, 677–678.

13 Xu, R. R.; Pang, W. Q.; Yu, J. H.; Huo, Q. S.; Chen, J. S. *Chemistry of Zeolites and Related Porous Materials*; John Wiley & Sons, Ltd: Singapore, 2007.

14 Kirschhock, C. E. A.; Buschmann, V.; Kremer, S.; Ravishankar, R.; Houssin, C. J. Y.; Mojet, B. L.; van Santen, R. A.; Grobet, P. J.; Jacobs, P. A.; Martens, J. A. Zeosil Nanoslabs: Building Blocks in Npr(4)N(+)-Mediated Synthesis of Mfi Zeolite. *Angew. Chem., Int. Ed.* **2001**, *40*, 2637–2640.

15 Kirschhock, C. E. A.; Kremer, S. P. B.; Vermant, J.; Tendeloo, G. V.; Jacobs, P. A.; Martens, J. A. Design and Synthesis of Hierarchical Materials from Ordered Zeolitic Building Units. *Chem.—Eur. J.* **2005**, *11*, 4306–4313.

16 Francis, R. J.; Price, S. J.; Obrien, S.; Fogg, A. M.; Ohare, D.; Loiseau, T.; Ferey, G. Formation of an Intermediate During the Hydrothermal Synthesis of Ulm-5 Studied Using Time-Resolved, in Situ X-Ray Powder Diffraction. *Chem. Commun.* **1997**, 521–522.

17 Agger, J. R.; Pervaiz, N.; Cheetham, A. K.; Anderson, M. W. Crystallization in Zeolite a Studied by Atomic Force Microscopy. *J. Am. Chem. Soc.* **1998**, *120*, 10754–10759.

18 Norby, P. Hydrothermal Conversion of Zeolites: An in Situ Synchrotron X-Ray Powder Diffraction Study. *J. Am. Chem. Soc.* **1997**, *119*, 5215–5221.

19 Valtchev, V. P.; Bozhilov, K. N. Evidences for Zeolite Nucleation at the Solid-Liquid Interface of Gel Cavities. *J. Am. Chem. Soc.* **2005**, *127*, 16171–16177.

20 Francis, R. J.; O'Hare, D. The Kinetics and Mechanisms of the Crystallisation of Microporous Materials. *J. Chem. Soc., Daton Trans.* **1998**, 3133–3148.

21 Grandjean, D.; Beale, A. M.; Petukhov, A. V.; Weckhuysen, B. M. Unraveling the Crystallization Mechanism of CoAlPO-5 Molecular Sieves under Hydrothermal Conditions. *J. Am. Chem. Soc.* **2005**, *127*, 14454–14465.

22 Weckhuysen, B. M.; Baetens, D.; Schoonheydt, R. A. Spectroscopy of the Formation of Microporous Transition Metal Ion Containing Aluminophosphates under Hydrothermal Conditions. *Angew. Chem., Int. Ed.* **2000**, *39*, 3419–3422.

23 Li, C. Identifying the Isolated Transition Metal Ions/Oxides in Molecular Sieves and on Oxide Supports by UV Resonance Raman Spectroscopy. *J. Catal.* **2003**, *216*, 203–212.

24 Tanev, P. T.; Chibwe, M.; Pinnavaia, T. J. Titanium-Containing Mesoporous Molecular Sieves for Catalytic Oxidation of Aromatic Compounds. *Nature* **1994**, *368*, 321–323.

25 Tuel, A. Crystallization of Titanium Silicalite-1 (Ts-1) from Gels Containing Hexanediamine and Tetrapropylammonium Bromide. *Zeolites* **1996**, *16*, 108–117.

26 Scarano, D.; Zecchina, A.; Bordiga, S.; Geobaldo, F.; Spoto, G. Fourier-Transform Infrared and Raman Spectra of Pure and Al-, B-, Ti- and Fe-Substituted Silicalites: Stretching-Mode Region. *J. Chem. Soc., Faraday Trans.* **1993**, *89*, 4123–4130.

27 Lamberti, C.; Bordiga, S.; Zecchina, A.; Carati, A.; Fitch, A. N.; Artioli, G.; Petrini, G.; Salvalaggio, M.; Marra, G. L. Structural Characterization of Ti-Silicalite-1: A Synchrotron Radiation X-Ray Powder Diffraction Study. *J. Catal.* **1999**, *183*, 222–231.

28 Li, C.; Xiong, G.; Xin, Q.; Liu, J. K.; Ying, P. L.; Feng, Z. C.; Li, J.; Yang, W. B.; Wang, Y. Z.; Wang, G. R.; Liu, X. Y.; Lin, M.; Wang, X. Q.; Min, E. Z. UV Resonance Raman Spectroscopic Identification of Titanium Atoms in the Framework of TS-1 Zeolite. *Angew. Chem., Int. Ed.* **1999**, *38*, 2220–2222.

29 Li, C.; Xiong, G.; Liu, J. K.; Ying, P. L.; Xin, Q.; Feng, Z. C. Identifying Framework Titanium in TS-1 Zeolite by UV Resonance Raman Spectroscopy. *J. Phys. Chem. B* **2001**, *105*, 2993–2997.

30 Zhang, W. H.; Lu, J. Q.; Han, B.; Li, M. J.; Xiu, J. H.; Ying, P. L.; Li, C. Direct Synthesis and Characterization of Titanium-Substituted Mesoporous Molecular Sieve Sba-15. *Chem. Mater.* **2002**, *14*, 3413–3421.

31 Yu, J. Q.; Feng, Z. C.; Xu, L.; Li, M. J.; Xin, Q.; Liu, Z. M.; Li, C. Ti-MCM-41 Synthesized from Colloidal Silica and Titanium Trichloride: Synthesis, Characterization, and Catalysis. *Chem. Mater.* **2001**, *13*, 994–998.

32 Li, C. UV Raman Spectroscopic Studies on Transition Metal-Containing Microporous and Mesoporous Materials: Active Sites and Synthesis Mechanism In *From zeolites to porous MOF materials--the 40th anniversary of International Zeolite Conference: proceedings of the 15th International Zeolite Conference, Beijing, P.R. China, 12-*

17th August 2007; Xu, R., Gao, Z., Chen, J., Yan, W., Eds.; Studies in Surface Science and Catalysis, Vol. 170; Elsevier: Amsterdam, 2007; Part 1; pp 561−576.

33 Long, R. Q.; Yang, R. T. Superior Fe-ZSM-5 Catalyst for Selective Catalytic Reduction of Nitric Oxide by Ammonia. *J. Am. Chem. Soc.* **1999**, *121*, 5595–5596.

34 Yoshizawa, K.; Shiota, Y.; Yamabe, T. Reaction Pathway for the Direct Benzene Hydroxylation by Iron-Oxo Species. *J. Am. Chem. Soc.* **1999**, *121*, 147–153.

35 Feng, X.; Keith Hall, W. FeZSM-5: A Durable SCR Catalyst for NOx Removal from Combustion Streams. *J. Catal.* **1997**, *166*, 368–376.

36 Sun, K. J.; Fan, F. T.; Xia, H. A.; Feng, Z. C.; Li, W.-X.; Li, C. Framework Fe Ions in Fe-ZSM-5 Zeolite Studied by UV Resonance Raman Spectroscopy and Density Functional Theory Calculations. *J. Phys. Chem. C* **2008**, *112*, 16036–16041.

37 Zhang, W. H.; Lu, J.; Han, B.; Li, M.; Xiu, J.; Ying, Y. P.; Li, C. Direct Synthesis and Characterization of Titanium-Substituted Mesoporous Molecular Sieve SBA-15. *Chem. Mater.* **2002**, *14*, 3413–3421.

38 Li, Y.; Feng, Z. C.; Lian, Y. X.; Sun, K. Q.; Zhang, L.; Jia, G. Q.; Yang, Q. H.; Li, C. Direct Synthesis of Highly Ordered Fe-SBA-15 Mesoporous Materials under Weak Acidic Conditions. *Microporous Mesoporous Mater.* **2005**, *84*, 41–49.

39 Li, Y.; Feng, Z. C.; Xin, H. C.; Fan, F. T.; Zhang, J.; Magusin, P.; Hensen, E. J. M.; van Santen, R. A.; Yang, Q. H.; Li, C. Effect of Aluminum on the Nature of the Iron Species in Fe-SBA-15. *J. Phys. Chem. B* **2006**, *110*, 26114–26121.

40 Galeener, F. L. Planar Rings in Glasses. *Solid State Commun.* **1982**, *44*, 1037–1040.

41 Fan, F. T.; Sun, K. J.; Feng, Z. C.; Xia, H. A.; Han, B.; Lian, Y. X.; Ying, P. L.; Li, C. From Molecular Fragments to Crystals: A UV Raman Spectroscopic Study on the Mechanism of Fe-ZSM-5 Synthesis. *Chem.—Eur. J.* **2009**, *15*, 3268–3276.

42 Li, M. J.; Feng, Z. C.; Xiong, G.; Ying, P. L.; Xin, Q.; Li, C. Phase Transformation in the Surface Region of Zirconia Detected by UV Raman Spectroscopy. *J. Phys. Chem. B* **2001**, *105*, 8107–8111.

43 Zhang, J.; Li, M. J.; Feng, Z. C.; Chen, J.; Li, C. UV Raman Spectroscopic Study on TiO_2. I. Phase Transformation at the Surface and in the Bulk. *J. Phys. Chem. B* **2006**, *110*, 927–935.

44 Fan, F. T.; Feng, Z. C.; Sun, K. J.; Guo, M. L.; Guo, Q.; Song, Y.; Li, W.-x.; Li, C. In Situ UV Raman Spectroscopic Study on the Synthesis Mechanism of AlPO-5. *Angew. Chem., Int. Ed.* **2009**, *48*, 8743–8747.

45 Fan, F. T.; Feng, Z. C.; Li, G. N.; Sun, K. J.; Ying, P. L.; Li, C. In Situ UV Raman Spectroscopic Studies on the Synthesis Mechanism of Zeolite X. *Chem.—Eur. J.* **2008**, *14*, 5125–5129.

46 Twu, J.; Dutta, P. K.; Kresge, C. T. Raman Spectroscopic Studies of the Synthesis of Faujasitic Zeolites Comparison of 2 Silica Sources. *Zeolites* **1991**, *11*, 672–679.

47 Maston, D. W.; Sharma, S. K.; Philpotts, J. A. Raman Spectra of Some Tectosilicates and of Glasses along the Orthoclase-Anorthite and Nepheline-Anorthite Joins. *Am. Mineral.* **1986**, *71*, 694–704.

48 McMillan, P. Structural Studies of Silicate Glasses and Melts Applications and Limitations of Raman Spectroscopy. *Am. Mineral.* **1984**, *69*, 622–644.

49 Dutta, P. K.; Puri, M. Synthesis and Structure of Zeolite ZSM-5: A Raman Spectroscopic Study. *J. Phys. Chem.* **1987**, *91*, 4329–4333.

50 McKeown, D. A.; Galeener, F. L.; Brown, J. Raman Studies of Al Coordination in Silica-Rich Sodium Aluminosilicate Glasses and Some Related Minerals. *J. Non-Cryst. Solids* **1984**, *68*, 361–378.